THE JOURNAL OF PHYSICAL CHEMISTRY B

Article

pubs.acs.org/JPCB

Development of AMOEBA Force Field for 1,3-Dimethylimidazolium Based Ionic Liquids

Oleg N. Starovoytov,* Hedieh Torabifard, and G. Andrés Cisneros*

Department of Chemistry, Wayne State University, Detroit, Michigan 48202, United States

Supporting Information

ABSTRACT: The development of AMOEBA (a multipolar polarizable force field) for imidazolium based ionic liquids is presented. Our parametrization method follows the AMOEBA procedure and introduces the use of QM intermolecular total interactions as well as QM energy decomposition analysis (EDA) to fit individual interaction energy components. The distributed multipoles for the cation and anions have been derived using both the Gaussian distributed multipole analysis (GDMA) and Gaussian electrostatic model-distributed multipole (GEM-DM) methods.[1] The intermolecular interactions of a 1,3-dimethylimidazolium [dmim$^+$] cation with various anions, including fluoride [F^-], chloride [Cl^-], nitrate [NO_3^-], and tetraflorouborate [BF_4^-], were studied using quantum chemistry calculations at the MP2/6-311G(d,p) level of theory. Energy decomposition analysis was performed for each pair using the restricted variational space decomposition approach (RVS) at the HF/6-311G(d,p) level. The new force field was validated by running a series of molecular dynamic (MD) simulations and by analyzing thermodynamic and structural properties of these systems. A number of thermodynamic properties obtained from MD simulations were compared with available experimental data. The ionic liquid structure reproduced using the AMOEBA force field is also compared with the data from neutron diffraction experiment and other MD simulations. Employing GEM-DM force fields resulted in a good agreement on liquid densities ρ, enthalpies of vaporization ΔH_{vap}, and diffusion coefficients $D_{\pm}$ in comparison with conventional force fields.

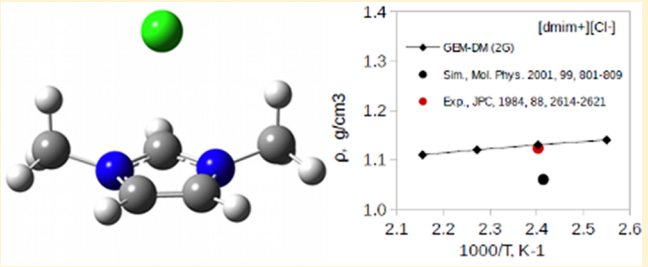

1. INTRODUCTION

The first ionic liquids (ILs) were introduced in the 1950s, with a significant increase in interest in the 1980s.[2] Room-temperature ionic liquids (RTILs) are organic salts with melting points below room temperature. Ionic liquids are a combination of asymmetric organic and inorganic ions that stay in a liquid phase over a wide temperature range. These ionic liquids are usually composed of organic cations and inorganic anions. The most studied are imidazolium$^+$, pyridinium$^+$, and pyrrolidinium$^+$ based cations in a combination with a broad number of anions. These cations are relatively easy to functionalize, and various types of side groups can be attached to obtain particular ionic liquid properties.

Thermodynamic properties such as low vapor pressure, excellent thermal and electrochemical stability, and good solvation properties make ionic liquids attractive for a wide range of applications. Practical applications can include materials for electrodeposition,[3] battery electrolytes,[4] and applications for catalysis.[5] The desired properties can be achieved by choosing a particular cation/anion combination. Therefore, there is an essential need to determine the physical and chemical properties of ILs in order to optimize their usage.

There are a large number of cation/anion combinations, which makes experimental determination of properties an expensive and time-consuming process.[6] Therefore, molecular modeling has become a powerful tool to predict ionic liquid properties without conducting an experiment. It is also practical to carry out molecular dynamics simulations to get some fundamental understanding on ionic liquids' behavior and to improve predictive capabilities of computational models. However, accurate simulations are needed to facilitate investigations of ionic liquids. There have been many computational studies performed to model and simulate a wide range of ionic liquids.[7] A systematic improvement of the force fields for molecular dynamics simulations of various compounds is a viable process, since molecular dynamics simulations are becoming an essential tool for scientific research and investigations. A broad variety of molecular dynamics simulation packages are available for researchers.[8] However, predictive capabilities of that software mostly depend on the quality of the employed force fields.

Most conventional force fields for ILs use partial atomic charges to describe the electrostatic interactions of molecules. A number of nonpolarizable[9] and polarizable[10] force fields that are based on partial atomic charges have been successfully developed and employed for the simulation of various compounds. Despite the good agreement with the experiment for a number of properties, those force fields show some

Received: April 4, 2014
Revised: June 4, 2014
Published: June 5, 2014

dx.doi.org/10.1021/jp503347f | J. Phys. Chem. B 2014, 118, 7156−7166

inaccuracies for certain cases and do not fully account for the anisotropy of the electrostatic interactions or for the charge density penetration effects.[11]

In order to improve the description of electrostatic interactions, higher order multipoles can be employed. Some of us have introduced a Gaussian electrostatic model (GEM), which uses Hermite Gaussians to describe the molecular charge density. In addition, we have shown recently that it is possible to obtain distributed multipoles, which we call GEM-DM multipoles, to describe electrostatic interactions in the atomic multipole optimized energetics for biomolecular applications (AMOEBA)[12] potential.[1] Several force fields have been developed using the distributed multipole approach.[13] The advantage of distributed multipoles over partial atomic charges is that point multipoles provide a better description of the charge density anisotropy, compared with point charge models.[14] However, these models do not account for the charge penetration effects at short interatomic distances.[15] One way to take into account anisotropy of electrostatic interactions and charge penetration effects is to employ damping functions.[16] An alternative is to use a continuous description of the molecular charge densities. Recently, a continuous description of the charge densities was successfully implemented for molecular dynamics simulations of water.[17]

In this contribution, we present the development of the multipolar-polarizable AMOEBA force field for 1,3-dimethylimidazolium based ILs using GEM-DM multipoles. In section 2, we present the methods employed for the parametrization, including EDA analysis and comparison of the GEM-DM multipole results to the Gaussian distributed multipole analysis (GDMA) results. Subsequently, we describe the methodology of the force field development and the details for the molecular dynamics simulations based on the new parameters. Finally, section 3 details the results and discussion for MD simulations on the target.

2. METHODS

In this section, we describe the parameter fitting methodology beginning with the parametrization procedure by means of quantum mechanical (QM) intermolecular interaction and energy decomposition analysis. This is followed by the details of the QM intermolecular interaction calculations employed for the parametrization. Subsection 2.3 describes the distributed multipoles calculation. Subsequently, subsections 2.4 and 2.5 describe the parametrization of intra- and intermolecular interactions. The optimization procedure of van der Waals parameters is described in subsection 2.6.

2.1. Parametrization Details for AMOEBA Using QM EDA Data. Our parametrization procedure is modified from the conventional AMOEBA method[13c] by introducing the use of QM energy decomposition analysis (EDA) to improve the description of each available individual nonbonded term. We adopt all functional forms of the multipole based AMOEBA force field for the development. The functional form of the AMOEBA potential is given by eq 1.

$$U_{\text{Total}} = U_{\text{bond}} + U_{\text{angle}} + U_{\text{b}\theta} + U_{\text{out}} + U_{\text{torsion}} + U_{\text{Coul}} + U_{\text{Pol}} + U_{\text{vdW}} \quad (1)$$

where the valence functional potentials are described by the potentials due to distortion of bonds (U_{bond}), bends (U_{angle}), torsions (U_{torsion}), and out-of-plane deformations (U_{out}). There is a bond-angle coupling term ($U_{\text{b}\theta}$) to account for stretching and bending modes. These functional potentials have been described in detail[13c] and are beyond the scope of the current work. In this work, we mainly focus on intermolecular interactions that are described by the last three terms of the potential: U_{Coul}, U_{Pol}, and U_{vdW}.

Permanent multipoles have been fitted for each atomic site (i) based on the QM electron density matrix for each molecule. The fitting procedure is discussed in subsection 2.3. The multipole components include point charge (q), dipole (μ), and quadrupole (Q) terms. These components are represented by a polytensor M.[13c] The potential energy due to the interaction of the permanent multipoles is calculated using eq 2.

$$U_{\text{Coul}}(r_{ij}) = M_i^{\text{T}} T_{ij} M_j \quad (2)$$

where T_{ij} is a multipole interaction matrix, M is a polytensor, and r_{ij} is the distance between site i and site j. A detailed description of the interaction tensor T_{ij} can be found in ref 34.

The induced polarization is described by placing an inducible atomic polarizable point dipole moment, μ_i, on each interaction site. The induced dipoles are calculated as $\mu_i = \alpha_i E_i$, where α_i is the atomic polarizability and E_i is the external electric field. The polarizability interactions are damped at short range by means of the Thole scheme[18] to avoid the so-called "polarization catastrophe".[11] All atomic polarizabilites were adopted unchanged from the AMOEBA force field. The atomic polarizability values are given in the Supporting Information (S19). A test was performed on the sensitivity of the intermolecular polarization energies due to a variation of the damping parameter value α for the cation−cation and anion−anion pairs. Our results suggest that intermolecular interaction energies are insensitive to the change of the Thole exponent over the range of α = 0.08−0.45. Therefore, the Thole damping factor α with a value of 0.39 was used in calculations to be consistent with the AMOEBA force field. In previous studies, the Thole parameter was reduced to the value of 0.35 to get a better description of the polarization interactions for the canonical water dimer.[1]

The last term is the potential energy that arises due to van der Waals interactions. These interactions can be described by three functional forms.[19] van der Waals interactions are described by the buffered Halgren[19d] pairwise potential, as shown by eq 3.

$$U_{\text{vdW}}(r_{ij}) = \varepsilon_{ij}\left(\frac{1+0.07}{\left(\frac{r_{ij}}{R_{ij}^0}\right)+0.07}\right)^{14-7}\left(\frac{1+0.12}{\left(\frac{r_{ij}}{R_{ij}^0}\right)^7+0.12}-2\right) \quad (3)$$

where ε_{ij} is the potential well, r_{ij} is the separation distance between sites i and j, and R_{ij}^0 is the minimum energy interaction distance (radius) for sites i and j. This potential provides a better description for interaction of noble gases in comparison with other available potentials.[19d] The van der Waals parameters for the unlike atom types are calculated using a combining rule.[13c]

Validation of the developed force fields is performed by running a series of molecular dynamics simulations on ionic liquids and comparing essential thermodynamic properties with experimental data and other molecular dynamics simulation results. The fitting of van der Waals parameters can be

dx.doi.org/10.1021/jp503347f | J. Phys. Chem. B 2014, 118, 7156−7166

performed if necessary using a well-developed fitting methodology.[20]

2.2. Quantum Mechanical and Monomer AMOEBA Calculations. Quantum mechanical calculations were performed for a single [dmim$^+$] cation and [F^-], [Cl^-], [NO_3^-], and [BF_4^-] anions using the Gaussian 09 software package.[21] One-electron, relaxed densities were calculated at the MP2-(full)/6-311G(d,p) level of theory for all ions and ion pairs. Structures of isolated cations and anions were optimized using the same level of theory and basis set. This level of theory was chosen to remain consistent with the AMOEBA force field development methodology.[22] The absence of imaginary frequencies in harmonic vibrational calculations proved that optimized structures correspond to local minima of the energy landscape. There are three [dmim$^+$] conformers to be considered. We find the lowest energy conformer for isolated [dmim$^+$] at the MP2(full)/6-311G(d,p) level by the rotational isomerization of methyl groups. The lowest energy conformer has its methyl hydrogens aligned in the same plane and direction as the hydrogen atom of a middle (C2) carbon on the imidazolium ring; see the Supporting Information (S14). Electron−electron correlation effects were also studied at the HF, MP2, and DFT levels of theory. Dipole moments for the three [dmim$^+$] optimized conformations were compared with the dipole moments obtained at the MP2 level of theory and various basis sets (see the Supporting Information, S15).

Gas phase normal mode vibrations for isolated ions [NO_3^-] and [BF_4^-] were carried out using the VALENCE tool available in the TINKER[8f] simulation package. Vibrational frequencies from the force field were compared with frequencies obtained from QM calculations at the MP2(full)/6-311G(d,p) level of theory (see the Supporting Information, S20).

We have used two methods for the determination of distributed multipoles. The first involves the use of GEM-DM,[23] and the second relies on GDMA.[11,24] The reason for the use of two different multipole sets is to compare the newly developed GEM-DM multipoles to the GDMA multipoles originally employed in the AMOEBA force field. GEM-DM distributed multipoles were obtained by fitting to one-electron densities from *ab initio* calculations using a single optimized geometry as discussed below. Both analytical and numerical fitting methods are available for the fitting of the QM densities to Hermite Gaussians.[1] The GDMA atomic multipoles were derived using Stone's approach.[11,24]

Intermolecular interaction energies were calculated next as a function of intermolecular separation distances for all ionic pairs. Total intermolecular energies were calculated using the counterpoise correction to take into account the basis set superposition error (BSSE).[25] Energy decomposition analysis was performed for each pair using the restricted variational space (RVS) decomposition approach[26] at the HF/6-311G-(d,p) level of theory as implemented in the GAMESS[27] software package. The Coulomb intermolecular interactions were calculated with an in-house FORTRAN90 program that enables the use of *ab initio* densities for the calculation of the intermolecular Coulomb energies with any one-electron relaxed density matrix for each monomer.

Molecular mechanics (MM) calculations were performed using both AMBER[8a] and TINKER[8f] simulation packages to ensure a correct reproduction of ion pair optimized geometries, total potential energies, and intermolecular energies from both packages. We have calculated total intermolecular interaction energies and interaction energies by energy components. Excellent agreement between both packages was established in describing intra- and intermolecular interactions for all ionic pairs.

2.3. Distributed Multipoles. The fitting methodology to obtain the distributed multipoles from GEM has been previously described.[1,17] In short, the density fitting method is based on employing auxiliary Gaussian basis functions (ABS) to fit the one-electron relaxed density. There are few available auxiliary basis sets such as A1, A2, and A2DG that can be used in the fitting.[28] We use the A2DG auxiliary basis set to obtain Hermite coefficients for the [dmim$^+$] cation and the A2 auxiliary basis set to obtain Hermite coefficients for anions. A direct mapping has been shown between the elements of the multipole tensor and Hermite Gaussian coefficients hc_{tuv} which enables the direct calculation of distributed Cartesian point multipoles from the fitted Hermite coefficients.[29] In this work, the Hermite coefficient Λ_{tuv} has a highest angular moment of 2 ($t + u + v = 2$), which results in distributed multipoles with a highest angular moment of quadrupoles. In GEM, the Hermite spherical Gaussians are normalized to 1, which guarantees that Cartesian multipoles can be calculated as defined by eq 4.

$$hc_{tuv} = hc_{tuv} \int \Lambda_{tuv}\, \mathrm{d}r \tag{4}$$

where $\Lambda_{tuv} = (\alpha/\pi)^{3/2}(\partial/\partial x)^t(\partial/\partial y)^u(\partial/\partial z)^v e^{(-\alpha r^2)}$ is the Hermite Gaussian function.

Fitting of GDMA multipoles was accomplished for cation and polyatomic anions according to the well-established GDMA fitting procedure.[11,24] It should be mentioned that the fitting of the GEM-DM multipoles relies not only on the reproduction of molecular electronic densities but also on the reproduction of intermolecular energies arising from electrostatic interactions of ionic pairs.

In order to enable the rotation of the multipoles, we have to define local coordinate frames for each atom site (i). The definition of local frames for the cation and anions can be found in the Supporting Information (see Tables S1−S4). The local frames are defined following the formalism employed in TINKER.[8f] The frames for [dmim$^+$] cation are kept identical for both the GDMA and GEM-DM models, but the definitions of frames for anions vary for the GDMA and GEM-DM models.

Four sets of [dmim$^+$] multipoles have been fit to compare the overall accuracy of the force fields with and without intramolecular polarization effects. All four sets of multipoles are fit to a one-electron density matrix, as discussed in computational section 2.1. Intramolecular polarization was not taken into account for the first set while fitting. 1,3-Dimethylimidazolium was considered as a single polarizable group. These multipoles are referred to as GDMA (1G) and GEM-DM (1G) multipoles. The second set of multipoles is fit taking into account intramolecular polarization effects by defining two polarizable segments of [dmim$^+$] following the procedure described elsewhere.[30] The polarization segmentation allows us to fit permanent atomic multipoles that would include an intramolecular polarization contribution from the [dmim$^+$] conformational dependence. The first polarizable group (segment) is defined by the imidazolium ring and a second group is defined by the methyl groups. These groups account for mutual polarization by fitting permanent multipoles upon rotation of methyl groups. The fitted multipoles will be further referred to as GDMA (2G) and GEM-DM (2G) multipoles. However, no mutual polarization has been applied

dx.doi.org/10.1021/jp503347f | J. Phys. Chem. B 2014, 118, 7156−7166

for polyatomic anions. All anions are defined as a single polarizable group. The fitted multipoles vary only by the fitting methodology used and referred to GDMA and GEM-DM multipoles.

2.4. Intramolecular Interactions. All intramolecular parameters (bond, bend, torsions, and out-of-plane deformations) were initially taken from the original AMOEBA[12,30,31] force field including parameters for 1,3-dimethylimidazolium and anions. Atomic polarizabilities α and van der Waals (ε_{ij} and R^0_{min}) parameters were also taken from the AMOEBA force field. Specifically, intramolecular equilibrium parameters for bonds, bends, torsions, and out-of-plane deformations of 1,3-dimethylimidazolium were adopted from the 4-ethylimidazole compound. However, the AMOEBA force field was augmented with (C2−N−Cm−Hm) torsional parameters for the [dmim$^+$] cation. A potential energy surface was generated using a 10° scan step fit to the MP2/6-311G(d,p) level of theory to get the best description of the conformational energy for this model compound. Torsional profiles are given in Figure 1a.

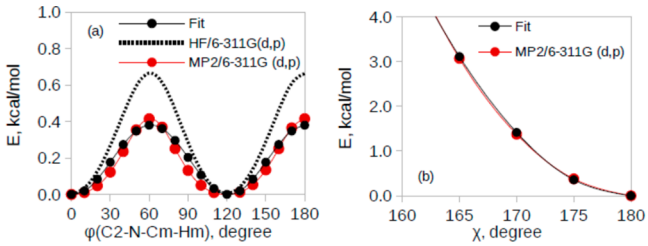

Figure 1. Conformational energy change for the C2−N−C−H torsion (a) and out-of-plane deformation for NO_3^- anion (b). MP2/6-311G(d,p) energies are red circles, HF/6-311G(d,p) energies are indicated by the dotted line, and the fit is indicated by black circles and a solid line.

Parameters for the (C2−N−Cm−Hm) torsion have been previously fit to the MP2/6-31+G(d) level by Liu et al. for the AMBER force field.[32] The torsional barrier is about 0.4 kcal/mol higher than the one obtained in our current calculations due to the smaller basis set used. However, we obtain a smaller rotational barrier using the HF/6-311G(d,p) level than the one reported by Liu et al. Nevertheless, we were unable to get a correct dimer optimized geometry in the gas phase with a torsional energy barrier of 0.9 kcal/mol. In contrast, Cadena and Maginn used C2−N−Cm−Hm with a torsional barrier of 0.195 kcal/mol.[7c] This barrier is too small in comparison with *ab initio* calculations. Intramolecular force field parameters for [dmim$^+$] are listed in the Supporting Information (S17) along with the parameters from QM calculations and X-ray experimental data.[33] It can be seen that the intramolecular parameters for the gas phase optimized geometry of [dmim$^+$] are in good agreement with both crystal structure and *ab initio* calculations.

We adopted equilibrium constants (k_0), bond lengths (r_0), and angles (θ_0) for [NO_3^-] from the parameters reported by Cadena and Maginn.[7c] van der Waals parameters were taken from amine nitrogen and amide oxygen as developed for the AMOEBA force field.[31] The optimized geometry of the [NO_3^-] anion is planar, which corresponds to the lowest energy state. Therefore, we fit the out-of-plane deformation constant (K_{out}) to ensure that the [NO_3^-] molecular model stays in the planar configuration; see Figure 1b. A good description of out-of-plane energies ($U_{out} = K_{out}\chi^2$) was obtained as compared with MP2/6-311G(d,p) calculations. Normal mode vibrational frequency analysis was performed next. The average unsigned difference was 119 cm^{-1}. We were not able to get a better agreement with QM calculations. The comparison of the gas phase vibrational energies from the force field and *ab initio* calculations for [NO_3^-] is given in the Supporting Information (Table S20-1).

Intramolecular parameters for [BF_4^-] were taken from the AMOEBA[12,30,31] force field. Normal mode vibrational analysis was also performed for this model compound. Good agreement in vibrational frequencies with *ab initio* and available experimental calculations was attained using AMOEBA parameters for the B−F bond and the F−B−F angle. The difference in asymmetric stretch was 192 cm^{-1}. The results of vibrational frequency analysis for BF_4^- anion are given in the Supporting Information (Table S20-2). Gas phase normal mode vibrations for [NO_3^-] and [BF_4^-] were carried out using the VALENCE tool available in TINKER.

2.5. Intermolecular Interactions. In order to calculate intermolecular interaction energies for ionic pairs, we use the same methodology implemented for nonionic compounds.[1,34] We systematically change the distance between cation center of mass and anion center of mass as shown in Figure 2 along the vector that is perpendicular to the plane of the [dmim$^+$] ring. In the case of [NO_3^-] and [BF_4^-], we use the same pathway as that for [F^-] and [Cl^-] varying the distance between the middle nitrogen and boron as shown. The total interaction energy in the gas phase was calculated at the MP2(full)/6-311G(d,p) level of theory with a step size of 0.2 Å using the optimized monomer geometries. The total intermolecular interaction energies were decomposed using the RVS decomposition analysis.[26] Energy decomposition analysis can

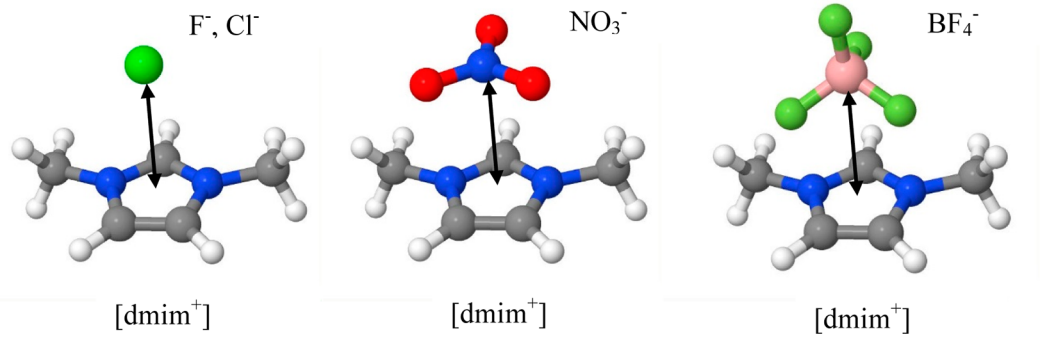

Figure 2. Schematic representations of ionic dimers, [dmim$^+$][F^-] and [dmim$^+$][Cl^-] (left), [dmim$^+$][NO_3^-] (middle), and [dmim$^+$][BF_4^-] (right). Arrows indicate the directions along which the anions were moved. Chemical structures were visualized employing jmol open software.[45]

dx.doi.org/10.1021/jp503347f | J. Phys. Chem. B 2014, 118, 7156−7166

be performed only at the HF level of theory. Therefore, we plotted intermolecular potentials from *ab initio* calculations using both MP2 and HF levels for comparison. The resulting intermolecular potential along with the corresponding energy components are given in Figure 3 for the [dmim$^+$][Cl$^-$] pair.

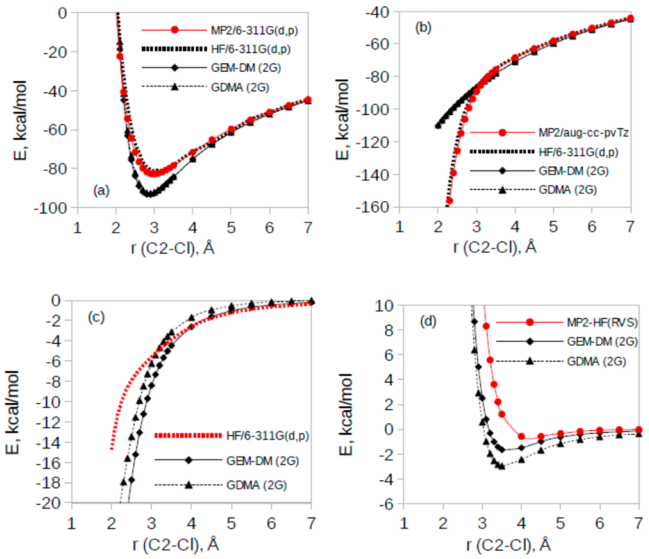

Figure 3. Comparison of interaction energies for the [dmim$^+$][Cl$^-$] ionic pair using GDMA and GEM-DM based force fields with *ab initio* data obtained at the MP2/6-311G(d,p) level: (a) total binding energy; (b) Coulomb energy; (c) polarization energy; (d) van der Waals energy.

Intermolecular potentials for other compounds are given in the Supporting Information (S21−S27). A good agreement on total intermolecular interactions is established using both the MP2 and HF levels. Intermolecular energies are systematically underestimated (∼1 kcal/mol) using the HF level for all pairs but [dmim$^+$][F$^-$] where the minimum energy is overestimated by ∼7 kcal/mol. We found the minimum interaction distance is at 3 Å for the [dmim$^+$][Cl$^-$] pair with a corresponding intermolecular energy of −82.81 kcal/mol. The intermolecular interaction distance is at 2.4 Å for the [dmim$^+$][F$^-$] pair with a minimum energy of −94.97 kcal/mol, which is more favorable than that for [dmim$^+$][Cl$^-$]. An interaction distance and a minimum energy for [dmim$^+$][NO_3^-] are comparable with those for [dmim$^+$][Cl$^-$]. The minimum interaction distance is 3.3 Å for [dmim$^+$][BF_4^-] with an energy of −79.95 kcal/mol, which is less favorable than energies for other compounds. These calculations indicate that intermolecular interactions become more favorable as the ion size decreases, and the interaction distances become shorter as the size of the anions becomes smaller as expected. The order for the intermolecular interaction energies can be placed as $E^{int}_{F^-} < E^{int}_{Cl^-} \approx E^{int}_{NO_3^-} < E^{int}_{BF_4^-}$. On the basis of these results, we expect to obtain a similar tendency on enthalpies of vaporization ΔH_{vap} for these model compounds. The highest energy of vaporization is expected for the [dmim$^+$][F$^-$] pair, and the lowest energy is expected for the [dmim$^+$][BF_4^-] pair.

Intermolecular energies are systematically overestimated employing both sets of force fields; see Figure 3a. The intermolecular energy minimum is overestimated by ∼9 kcal/mol using one group multipoles (1G) and by ∼6 kcal/mol using two group multipoles (2G) for the [dmim$^+$][Cl$^-$] ionic pair. Better agreement in the minimum energies is obtained for all other ionic compounds. Next, we perform energy decomposition analysis and plot intermolecular energies due to permanent multipoles U_{Coul}, induced polarization U_{Pol}, and van der Waals interactions U_{vdW} using both sets of force fields and compare those energies with the ones from the reference *ab initio* calculations.

Intermolecular Coulomb interactions are shown in Figure 3b. Intermolecular electrostatic interactions are well described by both sets of permanent multipoles at medium and long range. The multipoles with intramolecular induced polarization (2G sets) slightly overestimate the electrostatic interactions. A better description of intermolecular electrostatic interactions is attained using one group based multipoles as compared to the reference energies. We can see a greater deviation of electrostatic energies at short intermolecular distances. These energy deviations arise since the current version of these force fields does not account for the charge penetration effects. These effects can be included by means of damping functions.[16b,35]

The largest deviation between the AMOEBA force fields and the *ab initio* reference comes from the energies due to the polarization interactions U_{Pol}; see Figure 3c. GDMA (2G) tends to underestimate the polarization energies, while the forced fields based on only one polarization group tend to overestimate intermolecular energies for all ionic pairs as compared to the energies from HF/6-311G(d,p) calculations. The maximum energy difference between GDMA and GEM-DM based force fields is ∼1.2 kcal/mol. The potential energy $U_{Coul(MP2)}$ due to electrostatic interactions was calculated using an in-house FORTRAN90 program. The polarization interaction, $U_{Pol(HF)}$, was calculated using the RVS method.

Intermolecular energies due to van der Waals interactions are given in Figure 3d. van der Waals parameters were taken directly from the AMOEBA force field. Reference van der Waals energies were calculated as the difference between total intermolecular energies at the MP2 level and the Coulomb energies due to permanent multipoles, and the energies due to polarization interactions as given by eq 5.

$$U_{vdW} = U_{Total(MP2)} - U_{Coul(MP2)} - U_{Pol(HF)} \quad (5)$$

A comparison of van der Waals energies using GDMA and GEM-DM reveals that both potentials are more attractive as compared to *ab initio* calculations. The van der Waals interactions are shifted to shorter interatomic distances for all ionic pairs except for the [dmim$^+$][F$^-$] pair; see the Supporting Information (S21−S27). A better agreement of van der Waals interactions is reached for [dmim$^+$][F$^-$] using the GEM-DM (2G) force field. However, the GDMA based force fields overestimate the van der Waals interactions at short and long interaction distances while the GEM-DM based force fields show good agreement at long range. As noted above, the total intermolecular interactions calculated with both GEM-DM and GDMA based force fields show good agreement with the QM reference. This is due to a cancelation of errors between the overestimation of the van der Waals and polarization terms and the underestimation of the Coulomb term at short range.

One way to test the accuracy of the intermolecular interactions is by calculating the optimized geometries for the gas phase dimers. We performed geometry optimizations for all ionic pairs in the gas phase and compared geometries and corresponding energies with the ones obtained from *ab initio* calculations at the MP2/6-311G(d,p) level of theory; see the Supporting Information (S29−S32). Almost all optimized

dx.doi.org/10.1021/jp503347f | J. Phys. Chem. B 2014, 118, 7156−7166

geometries are well reproduced by both sets of force fields with the exception of the [dmim$^+$][F$^-$] pair, which optimizes to a different geometry as compared with *ab initio* results. In general, the GDMA based force fields have a tendency to underestimate the intermolecular interactions of the gas-phase dimers, while the GEM-DM based force fields show the opposite trend. These optimized geometries also show that the calculated parameters reproduce not only the potential energy surface (PES) for which they were parametrized but also those for other structures along the PES. This can be seen for four [dmim$^+$][Cl$^-$] dimers in different orientations; see the Supporting Information (S32).

2.6. van der Waals Parameter Fitting. We have previously developed a method for the efficient optimization of van der Waals parameters.[20] This method allows the combination of QM and experimental data for the optimization of van der Waals parameters by means of an active-space optimization approach with quadratic convergence. In the case of the ion pairs used in the current study, the only experimental data available is liquid density for [dmim$^+$][Cl$^-$]. Therefore, in this particular instance, we were unable to employ the active-space optimization approach due to the lack of experimental data in the literature. Initially, we have used an original set of van der Waals parameters for [dmim$^+$] and [Cl$^-$] and these parameters were optimized to match the available experimental data.

Our results indicate that both the GEM-DM and GDMA force fields slightly underestimate the liquid density of [dmim$^+$][Cl$^-$] (ρ = 1.08 g/cm^3) compared to the experimental data (1.123 g/cm^3)[36] and other molecular dynamics simulation results (1.06 g/cm^3)[37] at 425 K. In comparison, the density of the crystal is 1.281 g/cm^3.[33] Analysis of the van der Waals interactions reveals that our force fields are more attractive than the van der Waals energy obtained by the reference *ab initio* calculations at the MP2 level (see Figure 4). In this case, we

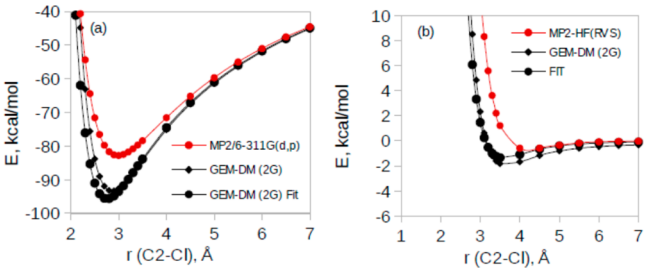

Figure 4. Total intermolecular energies (a) and van der Waals energies (b) before and after the fitting of van der Waals parameters for [dmim$^+$][Cl$^-$] employing the GEM-DM (2G) force field.

have relied on the scaling of the van der Waals radius R^0_{min} only for the cross terms of C−Cl, N−Cl, and H−Cl intermolecular interactions. To improve the description of the bulk properties with respect to the available experimental data for [dmim$^+$][Cl$^-$], the R^0_{min} interaction parameters have been rescaled for the GEM-DM (2G) force field in such a way so as to minimize the difference between experiment and simulation results for liquid density of the objective function $F(R^0_{min,i}) = \min \sum(\rho_{exp} - \rho_i)^2$.

After scaling the interatomic radii, the liquid density at 425 K shows a marked improvement with respect to the experimental result (1.127 g/cm^3). Liquids become denser at all other simulated temperatures. As can be seen in Figure 4, the energies due to van der Waals interactions are shifted to the shorter intermolecular distances, making the force fields even more attractive. This shift to lower energies may be due to the fact that the parameters are fitted to an intermediate level of theory (MP2/6-311G(d,p)). Recent force fields for different molecules fitted only to QM data at a higher level of theory have shown very good agreement with the experiment.[38] In a future contribution, we plan to employ a higher level of theory and more orientations for the ionic dimers to fit a larger set of ionic pairs.

2.7. Molecular Dynamics Simulation Methodology. Molecular dynamics (MD) simulations were performed for each ionic liquid pair using the AMBER12[39] simulation package. The AMOEBA force field was used to carry out MD simulations using a cubic simulation cell with applied periodic boundary conditions. The ionic liquid systems were set up on a periodic SC lattice that included 216 ionic pairs (3672−4536 atoms depending upon the system). Energy minimization was performed using the conjugate gradient minimization algorithm to reduce energetic strains. Simulations were carried out in the NVT ensemble to heat up the system to 600 K. The cutoff radius was 8.5 Å for nonbonded and electrostatic interactions. Isobaric−isothermal simulations were performed next until steady state conditions were reached with an integration time step of 1 fs. The Beeman integration algorithm[40] was employed for integrating equations of motion. Long-range electrostatic interactions were computed employing the smooth particle mesh Ewald method[41] with an 8 Å direct cutoff. The Berendsen thermostat and barostat[42] were used to control temperature and pressure with a relaxation time of 2.0 ps. Sampling trajectories were generated for 8 ns.

3. SIMULATION RESULTS

Molecular dynamics simulations were performed to demonstrate the accuracy of the newly developed AMOEBA force fields. Specifically, after implementing GDMA and GEM-DM multipoles and associated parameters, we obtain a good agreement (1% deviation) with the experimental result on liquid densities, ρ, after optimization of the van der Waals parameters for [dmim$^+$][Cl$^-$]. We also calculated enthalpies of vaporization ΔH_{vap} and diffusion coefficients $D_\pm$ as a function of temperature and compared the results with available MD simulation data from the literature. A summary of the data can be found in corresponding tables and the Supporting Information (S33−S41).

3.1. Ionic Liquid Volumes and Density. Volumes of ionic pairs are estimated at T = 425 K and are based on an average density from MD simulations. The volumes of [dmim$^+$][F$^-$] and [dmim$^+$][Cl$^-$] ion pairs were predicted to be 177.3 and 203.7 Å^3, respectively. Larger volumes were predicted for [dmim$^+$][NO$_3^-$] and [dmim$^+$][BF$_4^-$] as 223.5 and 241.5 Å^3, respectively; see Table 1. These results are well correlated with the anion radii where [F$^-$] is the smallest and tetrafluoroborate

Table 1. Liquid Volumes V at T = 425 K

	V (Å^3)	
ILs	GDMA (2G)	GEM-DM (2G)
[dmim$^+$][F$^-$]	174.7	177.3
[dmim$^+$][Cl$^-$]	203.8	203.7
[dmim$^+$][NO$_3^-$]	224.0	223.5
[dmim$^+$][BF$_4^-$]		241.6

dx.doi.org/10.1021/jp503347f | J. Phys. Chem. B 2014, 118, 7156−7166

$[BF_4^-]$ is the largest among four studied anions. The volume of $[BF_4^-]$ is 18 Å^3 larger than the volume of $[NO_3^-]$ and 37.8 Å^3 larger than that of $[Cl^-]$.

Comparison of the MD simulation results with the experiment for liquid densities of $[dmim^+][Cl^-]$ is given in Figure 5. The only available experimental data for the ionic

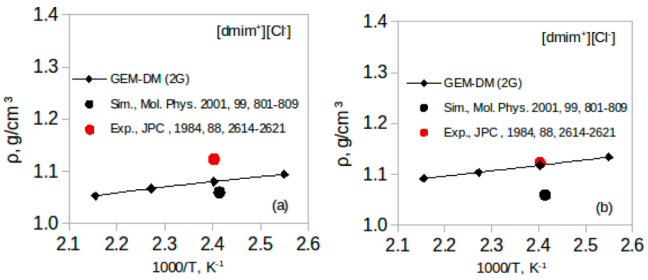

Figure 5. Comparison of liquid densities for $[dmim^+][Cl^-]$ employing GDMA and GEM-DM multipole force fields with experiment and other MD simulations: (left) liquid densities before the fitting of van der Waals interactions; (right) liquid densities after the fitting of van der Waals interactions.

liquid studied herein is for the liquid density of $[dmim^+][Cl^-]$ as mentioned above. Using the original van der Waals parameters, liquid densities of $[dmim^+][Cl^-]$ are 4% less than the experimental value at 425 K (see Figure 5a). However, after the van der Waals parameters are scaled, the GEM-DM (2G) force field shows very good agreement with the experiment with the error below 1%, as shown in Figure 5b and Table 2.

Table 2. Liquid Densities ρ at T = 425 K

	ρ (g/cm^3)		
ILs	GDMA (2G)	GEM-DM (2G)	experiment[36,43]
$[dmim^+][F^-]$	1.105	1.087	
$[dmim^+][Cl^-]$	1.082	1.118 (1.127)[a]	1.123
$[dmim^+][NO_3^-]$	1.179	1.181	
$[dmim^+][BF_4^-]$	1.370	1.265	

[a]The density value in parentheses corresponds to data after scaling of van der Waals parameters.

Simulation results for other ionic liquids are in good agreement with the results from other MD simulations[37] for ionic liquids with the greater molecular volume cations. For instance, a liquid density of 1.198 g/cm^3 was predicted from simulations for $[dmim^+][BF_4^-]$, while a density of 1.206 g/cm^3 was predicted from experiment for $[emim^+][BF_4^-]$ at 393 K. We predict the liquid density for $[dmim^+][BF_4^-]$ at 400 K to be 1.284 g/cm^3. The resulting difference of 6% can be ascribed to the larger volume of the $[emim^+]$ cation. The liquid density of $[bmim^+][NO_3^-]$ was reported to be 1.092 kcal/mol at 393 K.[10c] MD simulations showed the liquid density to be 1.198 kcal/mol for $[dmim^+][NO_3^-]$ at 400 K consistent with the change in molecular volume of the cation as above. Some variance in liquid densities is observed between our various multipolar force fields based on the different multipoles or number of polarization groups (see Table 2). The maximum deviation can be as large as ~10%.

3.2. Intermolecular Structure. Liquid structures of ionic liquids are usually compared to X-ray[7j] scattering or neutron[43] diffraction experimental data. In particular, interionic correlations are well described by radial distribution functions and can be compared with the structural factor $S(Q)$ obtained from neutron diffraction.[43] Radial distribution functions (RDFs) were calculated for the four ionic liquids at T = 475 K. A summary of these structures for $[dmim^+][Cl^-]$ is shown in Figure 6. These figures include cation−cation (C2−C2),

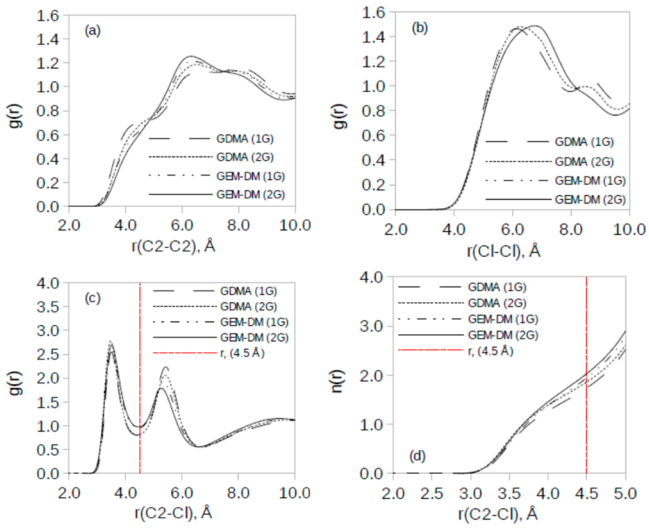

Figure 6. Comparison of intermolecular cation−cation (a), anion−anion (b), and cation−anion (c) radial distribution functions for $[dmim^+][Cl^-]$ employing GDMA and GEM-DM multipole force fields. The coordination number $n(r)$ is given for the cation−anions coordination shell (d). The red dotted line indicates the defined coordination shell.

cation−anion (C2−Cl^-), and anion−anion (Cl^-−Cl^-) interatomic correlations. Qualitatively similar results were obtained for all ionic liquids studied (see the Supporting Information). A typical correlation is observed for the ionic liquid structures as compared to the RDFs from other molecular dynamics simulations.[7c,d,i] The first peak of the coordination shell is shifted to longer distances as the ionic pairs change from $[dmim^+][F^-]$ to $[dmim^+][BF_4^-]$. These results are in good agreement with the results from gas phase optimized geometries. As the size of the anions increases, the intermolecular equilibrium distance increases for the dimer optimized geometries. There is not a significant difference in C2−C2 radial distribution functions that were calculated for two sets of the force fields. The GEM-DM (2G) force field resulted in less structured correlations, as indicated by a smooth interatomic curve in comparison with RDF curves using other force fields (see Figure 6a). Other force fields show a correlation peak at 4.0 Å. Similar structures were obtained from *ab initio* molecular dynamics simulations.[7i] The first (C2−C2) correlation peak can be found at a distance of 6.2 Å. The g(C2−C2) radial distributions are in good agreement with the structural model that was fit to the data from neutron diffraction experiments[43] and other molecular dynamics simulation results.[7i] Despite the difference in the description of charge densities for partial point charges vs atomic multipoles, the structural differences are negligible in these particular correlations. Similar tendencies are shown for the (Cl^-−Cl^-) anion−anion interatomic correlations. The next structure is the cation−anion (C2−Cl^-) radial distribution; see Figure 6c. Sharper peaks are obtained using the GDMA based force fields, again indicating more structured correlations in comparison with the GEM-DM (2G) force field. The first peak

dx.doi.org/10.1021/jp503347f | J. Phys. Chem. B 2014, 118, 7156−7166

Table 3. Enthalpy of Vaporization ΔH_{vap} at T = 425 K

	ΔH_{vap} (kJ/mol)				
ILs	GDMA (1G)	GDMA (2G)	GEM-DM (1G)	GEM-DM (2G)	simulation
$[dmim^+][F^-]$	175.7	172.2	168.2	168.5	
$[dmim^+][Cl^-]$	159.4	157.0	154.6	145.3 (175.0)[a]	187.1[b]
$[dmim^+][NO_3^-]$	169.4	167.1	164.4	162.4	
$[dmim^+][BF_4^-]$			147.3	139.8	

[a]The enthalpy value in parentheses corresponds to data after scaling of van der Waals parameters. [b]Reference 32. T = 423 K.

of the radial distribution is at a distance of 3.5 Å. These results are well correlated to gas phase optimized geometries for the dimers of ionic liquids. The first peaks for the $[dmim^+][F^-]$ and $[dmim^+][BF_4^-]$ are at interatomic distances of 3.0 and 3.9 Å, respectively. Qualitatively similar two peak distributions were obtained from molecular dynamics simulations of $[bmim^+][PF_6^-]$ at 298 K.[7d] The results indicated that the first peak is located at 4.0 Å interatomic distance. We also calculate the coordination number $n(r)$ by integrating the C2−Cl^- radial distribution function. The coordination shell is defined by the dotted red line. It can be seen that the $[dmim^+]$ cation is coordinated by two anions on average. If we define the coordination shell at the distance of second minimum, then we can see that the $[dmim^+]$ cation will be coordinated by six to seven anions depending upon the force field and anion types; see the Supporting Information.

3.3. Enthalpy of Vaporization. We calculated the heat of vaporization to estimate the strength of intermolecular interactions for ionic pairs. The enthalpy of vaporization is calculated as the energy required to bring an ionic pair from the liquid to the gas phase. Gas phase simulations were carried out using stochastic molecular dynamics simulations of a single ionic pair at 425 K. Making an assumption of an ideal gas behavior, the enthalpy of vaporization was estimated using the following relation.

$$\Delta H_{vap} = \Delta E + \Delta PV \quad (6)$$

where ΔE is the difference between potential energies from gas (−106.8 kcal/mol) and liquid phases (−141.9 kcal/mol) and ΔPV is the volume difference at constant pressure. Enthalpies of vaporization are listed in Table 3. Higher energies of vaporization correspond to the ionic liquids with anions of smaller radii, indicating stronger intermolecular interactions. These results are consistent with the results for other pairwise potentials; see the Supporting Information. These potentials predict more favorable energies for $[dmim^+][F^-]$ by 13 kJ/mol than for $[dmim^+][Cl^-]$ or $[dmim^+][NO_3^-]$ and by 15 kJ/mol in comparison with $[dmim^+][BF_4^-]$.

The GDMA based force fields resulted in higher energies of vaporization compared to the GEM-DM based force fields. These results can be referred to the difference in describing van der Waals interaction energies. The GEM-DM based force field has a better agreement on van der Waals interactions with the quantum chemistry results, while the GDMA force field overestimates van der Waals interactions by ∼2 kcal/mol. The calculated enthalpy of vaporization for $[dmim^+][Cl^-]$ ionic liquid with GEM-DM (2G) is 145.3 kJ/mol, which is significantly lower than the result of 187.1 kJ/mol at 423 K from simulations using point charges. After the scaling of van der Waals parameters, the calculated enthalpy of vaporization is 175.0 kJ/mol, which is 29.7 kJ/mol more favorable. This error might arise due (at least in part) to intermolecular energy deviations in electrostatic and polarization interactions. However, the empirical adjustment of van der Waals parameters can also have a significant influence on the strength of intermolecular interactions (see Table 4).

Table 4. Intermolecular van der Waals Parameters for N−Cl^-, C−Cl^-, and H−Cl^- before and after the Fitting

		before fitting		after fitting	
atom type pair	atom class pair	R_{min} (Å)	ε (kcal/mol)	R_{min} (Å)	ε (kcal/mol)
N−Cl^-	62−12	3.942	0.174	3.842	0.174
C−Cl^-	63−12	3.970	0.169	3.870	0.169
H−Cl^-	64−12	3.740	0.599	3.640	0.599

An increase in enthalpy of vaporization was predicted to be ∼4.0 kJ/mol per one CH_2 group from simulations of imidazolium based ionic liquids.[10c] Extrapolation of simulation results for $[emim^+]$ and $[bmim^+]$ with $[BF_4^-]$ at 298 K would result in an enthalpy of vaporization of ∼130 kJ/mol for $[dmim^+][BF_4^-]$. This value would be too low. Nevertheless, $[dmim^+][BF_4^-]$ ionic liquid is more likely to be in a crystalline state at 298 K. We also calculated the enthalpy of vaporization at 400 K for $[dmim^+][BF_4^-]$ obtaining 148 kJ/mol employing the GEM-DM force field.

3.4. Ion Self-Diffusion Coefficients. The self-diffusion coefficient is another liquid property that reflects the quality of the force fields implemented in molecular dynamics simulations. The mobility of ionic species depends on many parameters including the geometrical structure, ion size, charge delocalization, and strength of intermolecular interactions.[7e,h] A minor effect has been observed on the ion self-diffusion coefficient due to a change in a conformational barrier (C2−N−C−C).[7e] Faster ionic diffusion is also achieved using polarizable force fields in comparison with nonpolarizable ones. Inclusion of many body interactions speeds up the ion diffusion. Here, we study the influence of multipolar force fields on self-diffusion coefficients of ionic species. We compare GDMA and GEM-DM based force fields with available simulation and experimental data. The ion self-diffusion coefficients were calculated using the Einstein relation[44]

$$D_{\pm} = \lim_{t\to\infty} \frac{\langle \mathrm{MSD}_{\pm}(t)\rangle}{6t} \quad (7)$$

where $\mathrm{MSD}_{\pm}(t)$ is the mean square displacement of the molecule center of mass, t is the time, and $\langle\ \rangle$ defines an ensemble average. During the molecular dynamics simulations, the ions moved around ∼1000 and ∼4000 $Å^2$ over the production runs corresponding to 400 and 475 K, respectively. This indicates that the diffusion regime has been reached, since the mean square displacement of an ion is clearly much larger than two ionic radii of gyration (R_g ∼2.79 Å). We fit the linear

dx.doi.org/10.1021/jp503347f | J. Phys. Chem. B 2014, 118, 7156−7166

equation ($m^*t + c$) to the mean square displacement (MSD(t)) in the diffusive regime from the production trajectories. Production trajectories were generated for over 8 ns. Calculated self-diffusion coefficients for the [dmim$^+$] cation and various anions are given in Figure 7. The trends in the self-diffusion

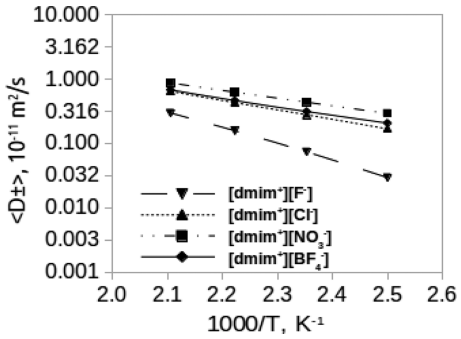

Figure 7. Comparison of self-diffusion coefficients $\langle D_{\pm} \rangle$ using the GEM-DM (2G) force field. Average self-diffusion coefficients are calculated for [dmim$^+$][F$^-$], [dmim$^+$][Cl$^-$], [dmim$^+$][NO$_3^-$], and [dmim$^+$][BF$_4^-$].

coefficients are well correlated with the enthalpies of vaporization. Borodin et al. have shown a correlation between enthalpy of vaporization and diffusion coefficients for a number of ionic liquids.[7h] We get similar relations, as faster diffusion rates are obtained for [dmim$^+$][NO$_3^-$] with lower enthalpy of vaporization in comparison with the [dmim$^+$][F$^-$] ionic liquid. However, we obtained lower diffusion rates for [dmim$^+$][BF$_4^-$] in comparison with [dmim$^+$][NO$_3^-$] despite having a lower enthalpy of vaporization. These results can be attributed to the geometry of [BF$_4^-$]. Previous studies have shown that the geometries of ions do have an impact on diffusion rates due to their weaker or stronger ordering.[7e]

The difference in diffusion rates between cations and anions is not significant. Diffusion rates reported by Borodin et al. for [emim$^+$][BF$_4^-$] using a polarizable force field[10c] are somewhat similar to [dmim$^+$][BF$_4^-$] using multipolar force fields. Therefore, the anisotropy of electrostatic interactions did not have a significant effect on the overall diffusion rates becoming comparable with the rates that result from employing partial charge based polarizable force fields.

4. CONCLUSIONS

We have developed AMOEBA polarizable force fields, that employ higher order multipoles to describe electrostatic interactions, for imidazolium based ionic liquids. The multipoles obtained by both the GDMA and the GEM-DM methods well describe intermolecular pair electrostatic interactions as compared to the energies from EDA analysis at medium and long range. A good description of the gas phase dimer geometries is also obtained without any empirical adjustments of the multipoles, atomic polarizabilities, or van der Waals parameters for all ionic liquids but [dmim$^+$][Cl$^-$]. The use of GDMA and GEM-DM multipoles in the newly developed AMOEBA force fields has shown initially a 4% deviation from experimental liquid densities ρ for [dmim$^+$][Cl$^-$]. The corresponding enthalpy of vaporization ΔH_{vap} is 145.3 kJ/mol. A limited number of experimental data is available for [dmim$^+$][Cl$^-$]. Therefore, empirical adjustments of the van der Waals parameters have been carried out only to experimental density. Excellent agreement was established in liquid densities (ρ = 1.127 g/cm^3) for [dmim$^+$][Cl$^-$] and an enthalpy of vaporization ΔH_{vap} of 175 kJ/mol after the optimization of the van der Waals parameters for this ion pair. Overall results indicate that the implementation of the GEM-DM (2G) force field has resulted in a good agreement in intermolecular energies as compared to QM calculations for all ionic liquids except for [dmim$^+$][Cl$^-$]. Thermodynamics and transport properties of the studied ionic liquids are in reasonable agreement with available data making the GEM-DM (2G) force field a good model to simulate 1,3-dimethylimidazolium based ionic liquids. Development of parameters for other anions and cations for simulations with the AMOEBA force field are currently underway.

■ ASSOCIATED CONTENT

Supporting Information

Definitions for all local frames, multipoles, and intra- and intermolecular interactions for [dmim$^+$][F$^-$], [dmim$^+$][NO$_3^-$], and [dmim$^+$][BF$_4^-$]. MD simulation results also given for these ionic liquids including densities ρ, enthalpies ΔH_{vap}, liquid structure $g(r)$, and self-diffusion coefficients $D_{\pm}$. This material is available free of charge via the Internet at http://pubs.acs.org.

■ AUTHOR INFORMATION

Corresponding Authors

*E-mail: oleg.starovoytov@wayne.edu.
*E-mail: andres@chem.wayne.edu.

Notes

The authors declare no competing financial interest.

■ ACKNOWLEDGMENTS

This research was supported by Wayne State University. Computing time from Wayne State University C&IT is gratefully acknowledged. The authors would like to thank the reviewers for insightful comments.

■ REFERENCES

(1) Cisneros, G. A. Application of Gaussian Electrostatic Model (GEM) Distributed Multipoles in the AMOEBA Force Field. *J. Chem. Theory Comput* **2012**, *8*, 5072−5081.
(2) Wilkes, J. S.; Levisky, J. A.; Wilson, R. A.; Hussey, C. L. Dialkylimidazolium Chloroaluminate Melts: A New Class of Room-Temperature Ionic Liquids for Electrochemistry, Spectroscopy and Synthesis. *Inorg. Chem.* **1982**, *21* (3), 1263−1264.
(3) Armand, M.; Endres, F.; MacFarlane, D. R.; Ohno, H.; Scrosati, B. Ionic-liquid materials for the electrochemical challenges of the future. *Nat. Mater.* **2009**, *8* (8), 621−629.
(4) Garcia, B.; Lavallée, S.; Perron, G.; Michot, C.; Armand, M. Room Temperature Molten Salts as Lithium Battery Electrolyte. *Electrochim. Acta* **2004**, *49* (26), 4583−4588.
(5) Olivier-Bourbigou, H.; Magna, L.; Morvan, D. Ionic Liquids and Catalysis: Recent Progress From Knowledge to Applications. *Appl. Catal., A* **2010**, *373* (1−2), 1−56.
(6) Zhang, S. J.; Sun, N.; He, X. Z.; Lu, X. M.; Zhang, X. P. Physical properties of ionic liquids: Database and evaluation. *J. Phys. Chem. Ref. Data* **2006**, *35* (4), 1475−1517.
(7) (a) Lopes, J. N. C.; Deschamps, J.; Padua, A. A. H. Modeling ionic liquids using a systematic all-atom force field. *J. Phys. Chem. B* **2004**, *108* (6), 2038−2047. (b) Lopes, J. N. C.; Padua, A. A. H. Molecular force field for ionic liquids composed of triflate or bistriflylimide anions. *J. Phys. Chem. B* **2004**, *108* (43), 16893−16898. (c) Cadena, C.; Maginn, E. J. Molecular simulation study of some thermophysical and transport properties of triazolium-based ionic liquids. *J. Phys. Chem. B* **2006**, *110* (36), 18026−18039. (d) Morrow, T. I.; Maginn, E. J. Molecular Dynamics Study of the

Ionic Liquid 1-n-Butyl-3-methylimidazolium Hexafluorophosphate. *J. Phys. Chem. B* **2002**, *106*, 12807−12813. (e) Hooper, J. B.; Starovoytov, O. N.; Borodin, O.; Bedrov, D.; Smith, G. D. Molecular dynamics simulation studies of the influence of imidazolium structure on the properties of imidazolium/azide ionic liquids. *J. Chem. Phys.* **2012**, *136* (19), 194506. (f) Borodin, O.; Smith, G. D. Structure and dynamics of N-methyl-N-propylpyrrolidinium bis-(trifluoromethanesulfonyl)imide ionic liquid from molecular dynamics simulations. *J. Phys. Chem. B* **2006**, *110* (23), 11481−90. (g) Borodin, O.; Smith, G. D.; Geiculescu, O.; Creager, S. E.; Hallac, B.; DesMarteau, D. Li+ transport in lithium sulfonylimide-oligo(ethylene oxide) ionic liquids and oligo(ethylene oxide) doped with LiTFSI. *J. Phys. Chem. B* **2006**, *110* (47), 24266−74. (h) Borodin, O. Relation between heat of vaporization, ion transport, molar volume, and cation-anion binding energy for ionic liquids. *J. Phys. Chem. B* **2009**, *113* (36), 12353−7. (i) Bühl, M.; Chaumont, A.; Schurhammer, R.; Wipff, G. Ab initio molecular dynamics of liquid 1,3-dimethylimidazolium chloride. *J. Phys. Chem. B* **2005**, *109* (39), 18591−18599. (j) de Andrade, J.; Boes, E. S.; Stassen, H. Computational study of room temperature molten salts composed by 1-alkyl-3-methylimidazolium cations-force-field proposal and validation. *J. Phys. Chem. B* **2002**, *106* (51), 13344−13351.

(8) (a) Case, D. A.; Cheatham, T. E., 3rd; Darden, T.; Gohlke, H.; Luo, R.; Merz, K. M., Jr.; Onufriev, A.; Simmerling, C.; Wang, B.; Woods, R. J. The Amber biomolecular simulation programs. *J. Comput. Chem.* **2005**, *26* (16), 1668−88. (b) Berendsen, H. J. C.; van der Spoel, D.; van Drunen, R. GROMACS: A Message-Passing Parallel Molecular Dynamics Implementation. *Comput. Phys. Commun.* **1995**, *91* (1−3), 43−56. (c) Van Der Spoel, D.; Lindahl, E.; Hess, B.; Groenhof, G.; Mark, A. E.; Berendsen, H. J. GROMACS: fast, flexible, and free. *J. Comput. Chem.* **2005**, *26* (16), 1701−18. (d) Plimpton, S. Fast Parallel Algorithms for Short-Range Molecular Dynamics. *J. Comput. Phys.* **1995**, *117*, 1−19. (e) Todorov, I. T.; Smith, W. DL_POLY_3: the CCP5 national UK code for molecular-dynamics simulations. *Philos. Trans.: Math., Phys. Eng. Sci.* **2004**, *362* (1822), 1835−52. (f) Ponder, J. W. *TINKER, Software Tools for Molecular Design*, version 5.0; Washington University: St. Louis, MO, 2004.

(9) (a) Schuler, L. D.; Daura, X.; Van Gunsteren, W. F. An Improved GROMOS96 Force Field for Aliphatic Hydrocarbons in the Condensed Phase. *J. Comput. Chem.* **2001**, *22* (11), 1205−1218. (b) McDonald, N. A.; Jorgensen, W. L. Development of an All-Atom Force Field for Heterocycles. Properties of Liquid Pyrrole, Furan, Diazoles, and Oxazoles. *J. Phys. Chem. B* **1998**, *102* (41), 8049−8059. (c) Jorgensen, W. L.; Maxwell, D. S.; Tirado-Rives, J. Development and Testing of the OPLS All-Atom Force Field on Conformational Energetics and Properties of Organic Liquids. *J. Am. Chem. Soc.* **1996**, *118* (45), 11225−11236. (d) Cornell, W. D.; Cieplak, P.; Bayly, C. I.; Gould, I. R.; Merz, K. M.; Ferguson, D. M.; Spellmeyer, D. C.; Fox, T.; Caldwell, J. W.; Kollman, P. A. A Second Generation Force Field for the Simulation of Proteins, Nucleic Acids, and Organic Molecules. *J. Am. Chem. Soc.* **1995**, *117* (19), 5179.

(10) (a) Borodin, O.; Smith, G. D. Development of many-body polarizable force fields for Li-battery applications: 2. LiTFSI-doped Oligoether, polyether, and carbonate-based electrolytes. *J. Phys. Chem. B* **2006**, *110* (12), 6293−9. (b) Borodin, O.; Smith, G. D. Development of many-body polarizable force fields for Li-battery components: 1. Ether, alkane, and carbonate-based solvents. *J. Phys. Chem. B* **2006**, *110* (12), 6279−92. (c) Borodin, O. Polarizable force field development and molecular dynamics simulations of ionic liquids. *J. Phys. Chem. B* **2009**, *113* (33), 11463−78.

(11) Stone, A. J. Distributed Multipole Analysis, or How to Describe a Molecular Charge Distribution. *Chem. Phys. Lett.* **1981**, *83* (2), 233−239.

(12) Ren, P.; Ponder, J. W. Polarizable Atomic Multipole Water Model for Molecular Mechanics Simulation. *J. Phys. Chem. B* **2003**, *107* (24), 5933−5947.

(13) (a) Gresh, N.; Cisneros, G. A.; Darden, T. A.; Piquemal, J. P. Anisotropic, Polarizable Molecular Mechanics Studies of Inter- and Intramolecular Interactions and Ligand-Macromolecule Complexes. A Bottom-Up Strategy. *J. Chem. Theory Comput* **2007**, *3* (6), 1960−1986. (b) Hermida-Ramon, J. M.; Brdarski, S.; Karlstrom, G.; Berg, U. Inter- and intramolecular potential for the N-formylglycinamide-water system. A comparison between theoretical modeling and empirical force fields. *J. Comput. Chem.* **2003**, *24* (2), 161−76. (c) Ponder, J. W.; Wu, C.; Ren, P.; Pande, V. S.; Chodera, J. D.; Schnieders, M. J.; Haque, I.; Mobley, D. L.; Lambrecht, D. S.; DiStasio, R. A., Jr.; Head-Gordon, M.; Clark, G. N.; Johnson, M. E.; Head-Gordon, T. Current status of the AMOEBA polarizable force field. *J. Phys. Chem. B* **2010**, *114* (8), 2549−64.

(14) (a) Kosov, D. S.; Popelier, P. L. A. Atomic Partitioning of Molecular Electrostatic Potentials. *J. Phys. Chem. A* **2000**, *104* (31), 7339−7345. (b) Popelier, P. L. A.; Joubert, L.; Kosov, D. S. Convergence of the Electrostatic Interaction Based on Topological Atoms. *J. Phys. Chem. A* **2001**, *105* (35), 8254−8261.

(15) Freitag, M. A.; Gordon, M. S.; Jensen, J. H.; Stevens, W. J. Evaluation of charge penetration between distributed multipolar expansions. *J. Chem. Phys.* **2000**, *112* (17), 7300−7306.

(16) (a) Cisneros, G. A.; Tholander, S. N.; Parisel, O.; Darden, T. A.; Elking, D.; Perera, L.; Piquemal, J. P. Simple Formulas for Improved Point-Charge Electrostatics in Classical Force Fields and Hybrid Quantum Mechanical/Molecular Mechanical Embedding. *Int. J. Quantum Chem.* **2008**, *108* (11), 1905−1912. (b) Piquemal, J. P.; Cisneros, G. A.; Reinhardt, P.; Gresh, N.; Darden, T. A. Towards a force field based on density fitting. *J. Chem. Phys.* **2006**, *124* (10), 104101. (c) Piquemal, J.-P.; Gresh, N.; Giessner-Prettre, C. Improved formulas for the calculation of the electrostatic contribution to intermolecular interaction energy from multipolar expansion of the electronic distribution. *J. Phys. Chem. B* **2003**, *107*, 10353−10359.

(17) Duke, R. E.; Starovoytov, O. N.; Piquemal, J. P.; G, C. A. GEM*: A Molecular Electronic Density-Based Force Field for Molecular Dynamics Simulations. *J. Chem. Theory Comput* **2014**, *10* (4), 1361−1365.

(18) Thole, B. T. Molecular polarizabilities calculated with a modified dipole interaction. *Chem. Phys.* **1981**, *59* (3), 341−350.

(19) (a) Lennard-Jones, J. E. Cohesion. *Proc. Phys. Soc., London* **1931**, *43* (5), 461−481. (b) Lennard-Jones, J. E.; S, F. R.; Devonshire, A. F. Critical Phenomena in Gases - I. *Proc. R. Soc. London, Ser. A* **1937**, *163*, 53−70. (c) Buckingham, R. A. The Classical Equation of State of Gaseous Helium, Neon, and Argon. *Proc. R. Soc. London, Ser. A* **1938**, *168*, 264−283. (d) Halgren, T. A. Representation of van der Waals (vdW) Interactions in Molecular Mechanics Force Fields: Potential Form, Combination Rules, and vdW Parameters. *J. Am. Chem. Soc.* **1992**, *114*, 7827−7843.

(20) Burger, S. K.; Cisneros, G. A. Efficient Optimization of van der Waals Parameters from Bulk Properties. *J. Comput. Chem.* **2013**, *34* (27), 2313−2319.

(21) Frisch, M. J.; Trucks, G. W.; Schlegel, H. B.; Scuseria, G. E.; Robb, M. A.; Cheeseman, J. R.; Scalmani, G.; Barone, V.; Mennucci, B.; Petersson, G. A.; Nakatsuji, H.; Caricato, M.; Li, X.; Hratchian, H. P.; Izmaylov, A. F.; Bloino, J.; Zheng, G.; Sonnenberg, J. L.; Hada, M.; Ehara, M.; Toyota, K.; Fukuda, R.; Hasegawa, J.; Ishida, M.; Nakajima, T.; Honda, Y.; Kitao, O.; Nakai, H.; Vreven, T.; Montgomery, J. A., Jr.; Peralta, J. E.; Ogliaro, F.; Bearpark, M.; Heyd, J. J.; Brothers, E.; Kudin, K. N.; Staroverov, V. N.; Kobayashi, R.; Normand, J.; Raghavachari, K.; Rendell, A.; Burant, J. C.; Iyengar, S. S.; Tomasi, J.; Cossi, M.; Rega, N.; Millam, J. M.; Klene, M.; Knox, J. E.; Cross, J. B.; Bakken, V.; Adamo, C.; Jaramillo, J.; Gomperts, R.; Stratmann, R. E.; Yazyev, O.; Austin, A. J.; Cammi, R.; Pomelli, C.; Ochterski, J. W.; Martin, R. L.; Morokuma, K.; Zakrzewski, V. G.; Voth, G. A.; Salvador, P.; Dannenberg, J. J.; Dapprich, S.; Daniels, A. D.; Farkas, O.; Foresman, J. B.; Ortiz, J. V.; Cioslowski, J.; Fox, D. J. *Gaussian 09*, revision A.02; Gaussian, Inc.: Wallingford, CT, 2010.

(22) Wu, J. C.; Chattree, G.; Ren, P. Automation of AMOEBA polarizable force field parameterization for small molecules. *Theor. Chem. Acc.* **2012**, *131* (3), 1138.

(23) (a) Cisneros, G. A.; Piquemal, J. P.; Darden, T. A. Intermolecular electrostatic energies using density fitting. *J. Chem. Phys.* **2005**, *123* (4), 044109. (b) Cisneros, G. A.; Piquemal, J. P.;

Darden, T. A. Generalization of the Gaussian electrostatic model: extension to arbitrary angular momentum, distributed multipoles, and speedup with reciprocal space methods. *J. Chem. Phys.* **2006**, *125* (18), 184101.
(24) Stone, A. J. Distributed Multipole Analysis: Stability for Large Basis Sets. *J. Chem. Theory Comput.* **2005**, *1* (6), 1128−1132.
(25) Stevens, W. J.; Fink, W. H. Frozen fragment reduced variational space analysis of hydrogen bonding interactions. Application to the water dimer. *Chem. Phys. Lett.* **1987**, *139* (1), 15−22.
(26) Kitaura, K.; Morokuma, K. A New Energy Decomposition Scheme for Molecular Interactions within the Hartree-Fock Approximation. *Int. J. Quantum Chem.* **1976**, *X*, 325−340.
(27) Boys, S. F.; Bernardi, F. The calculation of small molecular interactions by the differences of separate total energies. Some procedures with reduced errors. *Mol. Phys.* **1970**, *19* (4), 553−566.
(28) Andzelm, J.; Wimmer, E. Density functional Gaussian-type-orbital approach to molecular geometries, vibrations, and reaction energies. *J. Chem. Phys.* **1992**, *96* (2), 1280−1303.
(29) Challacombe, M.; Schwgler, E.; Almlof, J. *Modern developments in Hartree-Fock theory: Fast methods for computing the Coulomb matrix*; Word Scientific Inc.: Singapore, 1996.
(30) Ren, P.; Ponder, J. W. Consistent treatment of inter- and intramolecular polarization in molecular mechanics calculations. *J. Comput. Chem.* **2002**, *23* (16), 1497−506.
(31) Ren, P.; Wu, C.; Ponder, J. W. Polarizable Atomic Multipole-based Molecular Mechanics for Organic Molecules. *J. Chem. Theory Comput.* **2011**, *7* (10), 3143−3161.
(32) Liu, Z. P.; Huang, S. P.; Wang, W. C. A refined force field for molecular simulation of imidazolium-based ionic liquids. *J. Phys. Chem. B* **2004**, *108* (34), 12978−12989.
(33) Arduengo, A. J.; Dias, H. V. R.; Harlow, R. L.; Kline, M. Electronic Stabilization of Nucleophilic Carbenes. *J. Am. Chem. Soc.* **1992**, *114* (14), 5530−5534.
(34) Starovoytov, O. N.; Borodin, O.; Bedrov, D.; Smith, G. D. Development of a Polarizable Force Field for Molecular Dynamics Simulations of Poly (Ethylene Oxide) in Aqueous Solution. *J. Chem. Theory Comput.* **2011**, *7* (6), 1902−1915.
(35) Cisneros, G. A.; Tholander, S. N.-I.; Parisel, O.; Darden, T. A.; Elking, D.; Perera, L.; Piquemal, J.-P. Simple formulas for improved point-charge electrostatics in classical force fields and hybrid quantum mechanical/molecular mechanical embedding. *Int. J. Quantum Chem.* **2008**, *108* (11), 1905−1912.
(36) Fannin, A. A.; Floreani, D. A.; King, L. A.; Landers, J. S.; Piersma, B. J.; Stech, D. J.; Vaughn, R. L.; Wilkes, J. S.; Williams, J. L. Properties of 1,3-Dialkylimidazolium Chloride Aluminum-Chloride Ionic Liquids 0.2. Phase-Transitions, Densities, Electrical Conductivities, and Viscosities. *J. Phys. Chem.* **1984**, *88* (12), 2614−2621.
(37) Hanke, C. G.; Price, S. L.; Lynden-Bell, R. M. Intermolecular potentials for simulations of liquid imidazolium salts. *Mol. Phys.* **2001**, *99* (10), 801−809.
(38) (a) Babin, V.; Leforestier, V.; Paesani, F. Development of a "First Principles" Water Potential with Flexible Monomers: Dimer Potential Energy Surface, VRT Spectrum, and Second Virial Coefficient. *J. Chem. Theory Comput* **2013**, *9* (12), 5395−5403. (b) Donchev, A. G.; Galkin, N. G.; Pereyaslavets, L. B.; Tarasov, V. I. Quantum mechanical polarizable force field (QMPFF3): Refinement and validation of the dispersion interaction for aromatic carbon. *J. Chem. Phys.* **2006**, *125* (24), 244107. (c) Bukowski, R.; Szalewicz, K.; Groenenboom, G. C.; van der Avoird, A. Predictions of the Properties of Water from First Principles. *Science* **2007**, *315* (5816), 1249−1252.
(39) Case, D. A.; Darden, T. A.; Cheatham, T. E., III; Simmerling, C. L.; Wang, J.; Duke, R. E.; Luo, R.; Walker, R. C.; Zhang, W.; Merz, K. M.; Roberts, B.; Hayik, S.; Roitberg, A.; Seabra, G.; Swails, J.; Götz, A. W.; Kolossváry, I.; Wong, K. F.; Paesani, F.; Vanicek, J.; Wolf, R. M.; Liu, J.; Wu, X.; Brozell, S. R.; Steinbrecher, T.; Gohlke, H.; Cai, Q.; Ye, X.; Wang, J.; Hsieh, M.-J.; Cui, G.; Roe, D. R.; Mathews, D. H.; Seetin, M. G.; Salomon-Ferrer, R.; Sagui, C.; Babin, V.; Luchko, T.; Gusarov, S.; Kovalenko, A.; Kollman, P. A. *AMBER 12*; University of California: San Francisco, CA. http://ambermd.org/doc12/Amber12.pdf, 12; 2012.
(40) (a) Schofield, P. Computer simulation studies of the liquid state. *Comput. Phys. Commun.* **1973**, *5* (1), 17−23. (b) Beeman, D. Some multistep methods for use in molecular dynamics calculations. *J. Comput. Phys.* **1976**, *20* (2), 130−139.
(41) (a) Darden, T.; York, D.; Pedersen, L. Particle mesh Ewald: An N·log(N) method for Ewald sums in large systems. *J. Chem. Phys.* **1993**, *98* (12), 10089−10092. (b) Essmann, U.; Perera, L.; Berkowitz, M. L.; Darden, T.; Lee, H.; Pedersen, L. G. A smooth particle mesh Ewald method. *J. Chem. Phys.* **1995**, *103* (19), 8577. (c) Darden, T.; Perera, L.; Li, L.; Pedersen, L. New tricks for modelers from the crystallography toolkit: the particle mesh Ewald algorithm and its use in nucleic acid simulations. *Structure* **1999**, *7* (3), R55−60.
(42) Berendsen, H. J. C.; Postma, J. P. M.; van Gunsteren, W. F.; DiNola, A.; Haak, J. R. Molecular-Dynamics with Coupling to an External Bath. *J. Chem. Phys.* **1984**, *81* (8), 3684−3690.
(43) Hardacre, C.; Holbrey, J. D.; McMath, S. E. J.; Bowron, D. T.; Soper, A. K. Structure of molten 1,3-dimethylimidazolium chloride using neutron diffraction. *J. Chem. Phys.* **2003**, *118* (1), 273−278.
(44) Allen, M. P.; Tildesley, D. J. *Computer Simulations of Liquids*; Oxford University Press: New York, 1987.
(45) *Jmol: an open-source Java viewer for chemical structures in 3D*; http://www.jmol.org/.